

A Novel Benford-Based Approach for Detecting Statistical Anomalies in Precinct-Level Election Data

Philip Eigen¹, [ORCID: 0009-0001-5000-7396](https://orcid.org/0009-0001-5000-7396), **Steven J. Miller**² and
Kevin Dayaratna³

¹ Center for Statistical Modeling and Scientific Analysis in Policy, Advancing American Freedom, Washington, D.C., USA

² Department of Mathematics and Statistics, Williams College, Williamstown, MA, USA

³ Center for Statistical Modeling and Scientific Analysis in Policy, Advancing American Freedom, Washington, D.C, USA

Address for correspondence: Kevin Dayaratna, Center for Statistical Modeling and Scientific Analysis in Policy, Advancing American Freedom, 801 Pennsylvania Ave. NW, Washington, D.C., 20004.

E-mail: kevin@advancingamericanfreedom.com.

Phone: (+1) 615 870 4283.

Abstract: We introduce a novel extension of Benford's Law that shifts attention from leading digits to the joint distribution of final digit pairs in numerical data. Traditional Benford-based tests rely on first-digit frequencies and require observa-

tions to span several orders of magnitude, a condition frequently violated in precinct-level election returns. To overcome this limitation, we develop a formal probabilistic framework for analyzing the behavior of the last two digits under Benfordian assumptions, which we denote L2-BL 10. Within this framework, we derive closed-form expressions for digit-pair probabilities and establish convergence bounds toward their limiting uniform distribution, providing new theoretical results that extend the statistical foundations of Benford analysis beyond its classical first-digit form. We then show that precinct-level vote counts are well approximated by a discrete Weibull distribution, linking this theoretical development to realistic data-generating processes encountered in elections. Monte Carlo simulations and empirical illustrations using data from nine states in the 2016 and 2020 U.S. presidential elections demonstrate how the L2-BL 10 framework can be operationalized as a practical diagnostic for identifying anomalous digit behavior. The result is a method that is both theoretically grounded and directly applicable to election forensics in settings where standard Benford tests are not appropriate.

Key words: Benford’s Law, Digit Analysis, Elections, Election Forensics

1 Introduction

Especially in closely contested races, questions can arise regarding the integrity of American elections. Close outcomes have occurred in congressional ([Dickenson, 1984](#)), state ([Collection, 1840](#)), and local elections ([City of Forest Acres, 2021](#)), where narrow margins have prompted scrutiny and, at times, formal review.

A variety of statistical approaches have been developed to evaluate the integrity of elections, including methods rooted in number theory (Mebane Jr, 2006), Bayesian finite mixture modeling (Mebane Jr., 2023), and broader anomaly-detection techniques (Zhang et al., 2019). Among these, Benford’s Law—best known for its first-digit formulation—has received particularly sustained attention in the literature.

A naming convention for Benford’s Law based tests labels them by their digit of study with BL, short for Benford’s Law. This convention seems to have been started by Mebane Jr (2006). It was hyphenated by Castaneda (2010), and was extended by Anderson et al. (2022) to include the numerical base of study (e.g. L2-BL 10 for base-10 analysis of the last two digits, or 2-BL 3 for base-3 analysis of second digits).

The classic formulation of Benford’s Law evaluates whether the distribution of first digits in a dataset (1-BL10) conforms to a logarithmic decay pattern. While this framework has proven useful across diverse fields—from accounting and hydrology to genomics (Fiar et al., 2012; Geyer and Martí, 2012; Grammatikos and Papanikolaou, 2021; Nigrini and Miller, 2007)—it is generally not well suited to precinct-level election data, as noted by Mebane Jr (2006) and Anderson et al. (2022).

These shortcomings arise because classic applications of Benford’s Law are most effective when data span several orders of magnitude—an assumption that does not hold for precinct-level election returns. In response, researchers have proposed alternative approaches, such as examining second-digit distributions or transforming vote counts into other numerical bases prior to applying first-digit tests (Mebane Jr, 2006; Anderson et al., 2022).

We take a different approach. Instead of modifying the first-digit framework, we shift

attention to the behavior of the final two digits of vote counts (L2-BL 10). We derive closed-form expressions for the probability that these digits align under Benfordian assumptions and show how this probability behaves as sample size increases. This method yields a testable structure that is well suited to the scale and dispersion of precinct data. By establishing convergence bounds toward the uniform benchmark of $1/10$, the method provides both theoretical grounding and practical criteria for identifying anomalous patterns.

Utilizing the discrete Weibull framework introduced by [Anderson et al. \(2022\)](#), we extend Benford-based methods for electoral forensics. By focusing on the distributional behavior of final digit pairs, the approach provides a principled way to detect irregularities in precinct-level data that lack the order-of-magnitude variation required for traditional first-digit tests. This formulation retains the simplicity and interpretability of Benford-inspired diagnostics while addressing structural features unique to election returns. Because the method relies only on publicly available vote data and well-defined distributional assumptions, it is transparent, reproducible, and straightforward to implement.

2 Benford’s Analysis and Generalizations

Toward the end of the 1800s, Simon Newcomb ([Newcomb, 1881](#)) observed that pages of logarithm tables corresponding to numbers beginning with smaller leading digits—such as 1, 2, and 3—showed noticeably greater wear than those associated with larger digits. Several decades later, Frank Benford documented similar patterns across a wide range of datasets, including X-ray voltages, population figures, and river areas ([Benford, 1938](#)). These observations gave rise to what is now known as Benford’s

Law, which has since found applications across numerous disciplines, including geology, economics, computer science, accounting, and hydrology (Nigrini and Miller, 2007; Geyer and Martí, 2012; Grammatikos and Papanikolaou, 2021; Jolion, 2001; Arshadi and Jahangir, 2014; Villas-Boas et al., 2017).

In analyzing Benford data, the aspect of the data of most interest is the distribution of the significand. As a result, it is important to remember that we can write any $y > 0$ in scientific notation as

$$y = S_{10}(y)10^{k(y)}, \quad (2.1)$$

where $k(y)$ is an integer and the significand $S_{10}(y)$ satisfies $1 \leq S_{10}(y) < 10$; for example 246.01 is written as $2.4601 \cdot 10^2$, and the last two digits of the significand are 0 and 1 (and these are the fourth and fifth digits). A dataset is considered Benford if the significands have the following density:

$$f(x) = \begin{cases} \frac{1}{x \log(10)} & 1 \leq x < 10 \\ 0 & \text{otherwise} \end{cases}. \quad (2.2)$$

Thus the probability of observing a significand at most s is simply represented by the integral of $f(x)$ from 1 to $s + 1$. Therefore, the probability of a first digit being d is

$$\int_{x=d}^{d+1} f(x)dx = \frac{1}{\log(10)} \cdot \log(x) \Big|_d^{d+1} = \frac{\log(d+1) - \log(d)}{\log(10)}, \quad (2.3)$$

simplifying to:

$$\log_{10}(1 + 1/d), \quad (2.4)$$

the classical formulation of Benford’s Law. Drawing upon Equation 2.4, one can see that the probabilities decrease from roughly 30% for a first digit of 1 down to about 4.6% for a 9. Figure 1 visualizes the distribution of first digits.

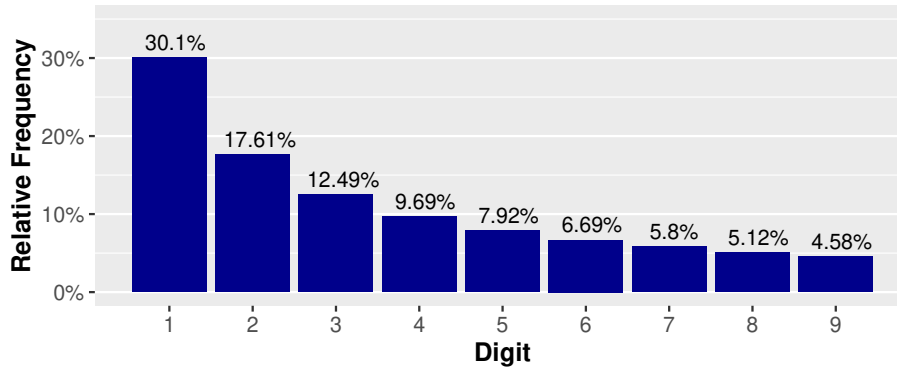


Figure 1: The Distribution of the Leading Digits According to Benford’s Law.

Although having some limitations, Benford analysis has been used extensively to study election integrity (Deckert et al., 2011; Mebane Jr, 2011). Mikoss (2004) was an early adopter, applying first-digit methods to the 2004 Venezuelan Recall Referendum, and Lakshmanan (2024) used them for the 2018 Russian Presidential Election. In 2006, Walter Mebane pointed out sensitivities in first-digit methods and suggested an alternative approach using the Benford’s Law distribution of the second digits (Mebane Jr, 2006), applying this approach to US, German, Russian, and Iranian elections (Mebane Jr, 2008, 2012, 2010).

It should be noted that while Benford’s Law traditionally applies to continuous data, it is often used for discrete data like counts (e.g. election forensics). What is important for Benford’s Law is that the significands of the data appear to be drawn from the interval $[1, 10) \subset \mathbb{R}$. When the data span multiple orders of magnitude, the significands of the dataset can appear to be functionally drawn from the continuum. For example, Miller (2015) uses county population sizes from the 2000 United States

Census to demonstrate Benford behavior in first digits. Despite the data being integer values, the magnitude and range of those values is such that their significands appear to be drawn from that interval. This reality is what makes application of Benford's Law to vote count data acceptable generally. That said, as is made clear in Section 3, our framework, unlike other Benford's Law based tests, does not require an a priori assumption of Benford conformity in the vote count data itself.

Several forms of Benford analysis have been used in analyzing the integrity of executive and legislative elections around the world. For example, [Pericchi and Torres \(2004\)](#) used 2-BL 10 for the Venezuelan 2004 Recall Referendum, [Jiménez and Hidalgo \(2014\)](#) used 2-BL 10 to look at a series of Venezuelan elections, [Beber and Scacco \(2012\)](#) used L1-BL 10 analysis for Nigerian and Senegalese elections, and [Anderson et al. \(2022\)](#) used a base-transformed version of first-digit analysis to look at a U.S. presidential election. While part of Beber's work did focus on final digits, this work takes some significant departures from that study. First, our focus on U.S. precinct-level data as opposed to election-specific scoping restricts the context such that assumptions regarding the applicability of Benford's Law can generally be observed to hold. Second, whereas the previous work primarily focused on direct comparisons to the expected behaviors as described, the development and employment of the Weibull modeling framework allows not only for more robust and flexible analysis, but for the automatic exclusion of cases which seem to diverge fundamentally from the assumptions.

A key problem with the first-digit representation of Benford's Law, however, is that the original law does not apply to clustered data, such as elections. This makes 1-BL 10 a weak or invalid test for such data. [Anderson et al. \(2022\)](#) applied an alteration

of Benford's Law by considering base 3 representations of precinct-level clustered election data. Benford's Law generalizes to an arbitrary base B as follows:

$$\begin{aligned} \text{Prob}(\text{First digit base } B \text{ is } d) &= \text{Prob}(\text{Significand base } B \text{ is in } [d, d+1)) \\ &= \log_B(d+1) - \log_B(d) = \log_B\left(\frac{d+1}{d}\right), \end{aligned}$$

While 1-BL 3 does largely address the issue of clustering by increasing the orders of magnitude over which the data span, the test can be hard to interpret for those who may wish to use it.

A number of papers have handled clustered data by considering probabilities associated with the second digit. The associated probabilities are as follows:

$$\begin{aligned} \text{Prob}(\text{Second digit is } d) &= \sum_{k=1}^9 [\log_{10}(k + (d+1)/10) - \log_{10}(k + d/10)] \\ &= \sum_{k=1}^9 \log_{10}\left(\frac{k + (d+1)/10}{k + d/10}\right) \\ &= \sum_{k=1}^9 \log_{10}\left(\frac{10k + d + 1}{10k + d}\right), \end{aligned} \tag{2.5}$$

and a similar calculation works to compute the probability of a digit of d in any fixed location. While second-digit tests reduce clustering effects, they remain sensitive when counts span only a narrow range, because early digits still deviate substantially from uniformity.

The chi-squared statistic is the most commonly used test to assess conformity to Benford's Law. For digits $d = 1, \dots, B - 1$, if $E(d)$ is the expected number that

have a first digit of d in base B , and $O(d)$ is the observed number of digits, then the associated chi-squared statistic is

$$\chi^2 = \sum_{d=1}^{B-1} \frac{(O(d) - E(d))^2}{E(d)}. \quad (2.6)$$

For 1-BL 3, there are only two possibilities for the leading digits. For a set that is Benford, we expect to observe a leading digit of 1 approximately 63.093% of the time and of 2 about 36.907%, with the chi-square values (with one degree of freedom) being 3.84 (at the 95% level) and 6.63 (at the 99% level).

In Section 4.1 we use findings from Theorem 1 to demonstrate that under Benford's Law, the probability of two consecutive digits being equal (or a "matched pair") approaches 1/10 as the ordinal location of those digits in the number grows. This result is the basis of our methodology as described in the next section. As such, $O(d)$ and $E(d)$ in our chi-squared tests take on the meaning of the observed and expected number of matched pairs, not particular digits. This gives our test statistics one degree of freedom.

3 Procedure for Applying L2-BL 10

Our framework for applying L2-BL 10 to counties' precinct-level vote count data consists of three steps. First, a distribution is fit to the data and the estimated distribution is tested for goodness-of-fit. Second, the fit distribution is assessed for conformity to Benford's Law via tests on samples as Monte Carlo simulations. Third, the county data is assessed for conformity to Benford's Law. We argue that if the fitted distribution provides an adequate baseline model for the county's counts, then

Benford-like behavior in Monte Carlo samples from that model provides evidence that the observed counts would also be expected to show Benford-like behavior under the baseline. Discrepancies between the observed data and this baseline expectation are treated as diagnostic flags that warrant further investigation. Thus, a county is flagged by this framework if the estimated distribution is well fit and the samples show general conformity to L2-BL 10, but the observed data does not conform to L2-BL 10.

As in past work on Benford’s Law based analysis of election data, we use a discrete Weibull distribution to model the skewed nature of precinct-level vote counts (Anderson et al., 2022). The discrete Weibull is capable of taking on many forms, and is commonly used to model highly skewed distributions (Nakagawa and Osaki, 1975) in a variety of settings (Englehardt and Li, 2011; Patriarca et al., 2019; Peluso et al., 2019). Often, the discrete Weibull is used for count data, as is the case in this work.

Precinct vote count distributions are modeled for each county and candidate. In particular, in county i with J precincts, candidate-specific precinct vote count, X_i , is modeled with probability mass function

$$P(X_i = x_{i,j}; \alpha_i, \beta_i) = \exp \left[- \left(\frac{x_{i,j}}{\alpha_i} \right)^{\beta_i} \right] - \exp \left[- \left(\frac{x_{i,j} + 1}{\alpha_i} \right)^{\beta_i} \right]$$

and cumulative mass function

$$P(X_i \leq x_{i,j}; \alpha_i, \beta_i) = 1 - \exp \left[- \left(\frac{x_{i,j} + 1}{\alpha_i} \right)^{\beta_i} \right],$$

where α is the scale parameter and β is the shape parameter. Letting $Y = \log(x + 1)$, $\mu = \log(\alpha)$, and $\sigma = \frac{1}{\beta}$, this CMF can be reformulated into a more familiar location-

scale parameterization (Stute et al., 1993). This parameterization will be the one used henceforth:

$$P(X_i \leq x_{i,j}; \alpha_i, \beta_i) = 1 - \exp \left[- \exp \left[\left(\frac{Y_{i,j} - \mu_i}{\sigma_i} \right) \right] \right].$$

Maximum likelihood estimation is used to find a best-fit discrete Weibull distribution by county and candidate, and one-sample, two-sided, discrete Kolmogorov-Smirnov (d-KS) tests assess goodness of fit.

Whereas the traditional KS test is limited to continuous distributions, Conover (1972) provided a combinatorial approach for calculating exact p-values for the one-sided d-KS test, and Gleser (1985) described how the work of Niederhausen (1981) on the continuous two-sided KS test based on rectangle probability of uniform order statistics can be applied to the discrete case. These calculations are very expensive, however, leading to numerical instability for sample sizes as small as 30. For d-KS p-values in cases of larger samples, some packages like `dgof` use asymptotic approximations or approximate based on the distribution of the standard KS test statistic, but these results are known to be conservative. The R package `KSgeneral`, written by the authors of the originating work Dimitrova et al. (2020), provides an alternative approach to calculating exact p-values for the two-sided d-KS test statistic. The otherwise prohibitive complexity of the problem is avoided via the authors' `exact-KS-FFT` method using fast Fourier transform.

However, while the d-KS test assumes a fully described null distribution, goodness-of-fit tests on null distributions with estimated parameters are known to have conservative results. Henze (1996) showed that in the case of tests based on estimated, discrete

null distributions under basic regularity conditions, parametric bootstrap tests based on the EDF asymptotically approach true power levels. Simulations in that study on the Poisson and Geometric distributions show that for the KS test, bootstrapping results in strong adherence to true test power even with small sample sizes. As such, the described procedure is used in this study to calculate d-KS p-values. Briefly stated, the procedure is as follows: the d-KS test statistic is calculated; samples are taken from the estimated distribution; new discrete Weibull parameters are calculated via MLE on the samples; d-KS statistics are calculated from the samples and their newly estimated distributions; the p-value is taken as the empirical probability of the original test statistic with respect to the bootstrap test statistics. In this study, we use 1000 bootstrap estimates for each county. In addition to greatly reducing the conservative effect of the estimated null distribution, this calculation avoids the risk of numerical instability from standard p-value calculation, instead adding only the time required to conduct the bootstrapping. An added benefit of this method is that unlike with a chi-squared test, there is no need for developing a heuristic for binning. Whereas that may be a simple issue for a unit of study with more homogeneous distributional behavior, the character of precinct-level vote count data, as expanded upon in Section 4.2, amplifies the issue the point of infeasibility for a test meant to be generally applicable.

Testing Benford conformity for the fitted distribution is done using the same chi-squared test used to assess Benford conformity in the observed data. It is a chi-squared test with one degree of freedom that compares the observed counts of matched-pairs and non-matched-pairs to their expected counts under Benford's Law. This is motivated by Definition 2.3.3 from [Berger and Hill \(2015\)](#). That definition, simplified, defines a random variable X as Benford if the probabilities of individual digits of X

are equal to those expected under Benford's Law. By running chi-squared tests on Monte Carlo samples, we provide a method of testing that behavior. Thus, with a null assumption of Benford conformity, a significant Monte Carlo p -value would imply that the digit probabilities are not the same as Benford's Law, so the distribution is not Benford. Likewise, a high Monte Carlo p -value would fail to reject the distribution's Benford conformity, thus allowing the assumption of Benford conformity to be applied to the observed data.

The full set of steps for applying L2-BL 10 analysis to elections are as follows.

- Use maximum likelihood estimation to fit a discrete Weibull to each county for each candidate.
- Conduct bootstrap d-KS tests between the data and the estimated distributions to assess goodness of fit.
- Assess the conformity of the estimated distributions to L2-BL 10 using chi-squared tests with repeated sampling as Monte Carlo simulations.
- Assess the conformity of the observed data to L2-BL 10 for each county and candidate using chi-squared tests.
- Record instances where a given county's estimated distribution is well fit to the data and conforms to L2-BL 10, but the observed data itself does not conform to L2-BL 10.

4 Methodological Support

In this section we will develop three points that combine to provide evidence for the validity of our framework. First, we will show the convergence of the probability of matched-pair digits to $1/10$, the null behavior we use to assess conformity to L2-BL 10. Second, we demonstrate the high performance of the discrete Weibull distribution when modeling precinct-level vote counts. Finally, we demonstrate that in most of the environment of parameterizations and sample sizes induced by precinct-level vote count data, the discrete Weibull distribution tends to produce samples conforming L2-BL 10.

4.1 The Probability of Matching Pairs Converges to $1/10$

While Benford's Law is most frequently applied with focus on the distribution of the first or second digits of a sequence of values, the law can be generalized to find the distribution of any arbitrary digit or combination of digits. In fact, as pointed out in Equation (2.3) from [Berger and Hill \(2015\)](#), Benford's Law can be described more completely as the joint probability

$$P((D_1, D_2, \dots, D_m) = (d_1, d_2, \dots, d_m)) = \log_{10} \left(1 + \left(\sum_{j=1}^m 10^{m-j} d_j \right)^{-1} \right) \quad (4.1)$$

for all positive integers m , where D_i is the i_{th} digit of the significand and $D_1 \geq 1$. As shown in Theorem 1, given Equation (4.1), Equation (2.5) can be further generalized for an arbitrary digit as

$$\text{Prob}(n_{\text{th}} \text{ digit is } d) = \sum_{k=10^{n-2}}^{10^{n-1}-1} \log_{10} \left(1 + \frac{1}{10k + d} \right). \quad (4.2)$$

Unlike the first digit's distribution, which rapidly decays across the first nine natural numbers, subsequent digits are considerably more evenly distributed, approaching uniformity as illustrated in Figure 2. The approach towards this limit is extremely quick and appears to take practical effect starting as early as the third or fourth digit.

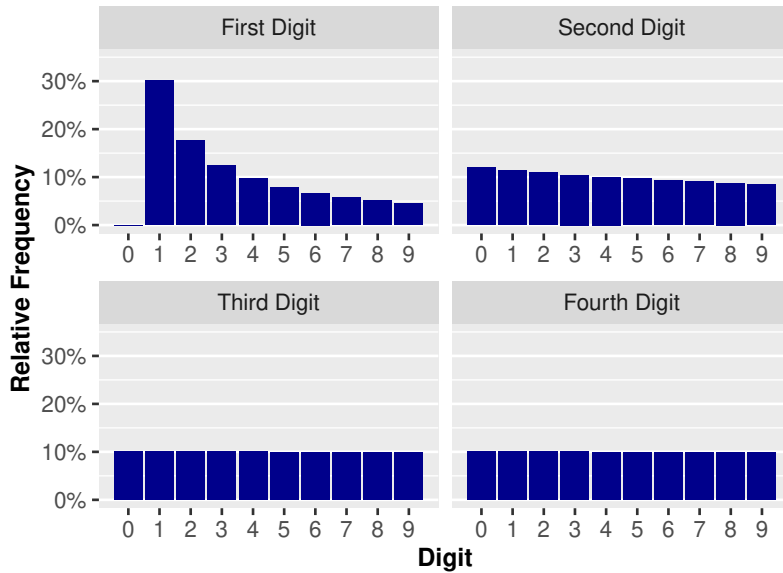


Figure 2: Digit Distributions Rapidly Approach Uniform, as Observed in the Distributions of the First Four Digits.

Theorem 1 goes on to show that we can also find the joint probability of D_n and D_{n+1} ,

$$P((D_n, D_{n+1}) = (d_n, d_{n+1})) = \sum_{k=10^{n-2}}^{10^{n-1}-1} \log_{10} \left(1 + \frac{1}{100k + 10d_n + d_{n+1}} \right), \quad (4.3)$$

and that

$$\lim_{n \rightarrow \infty} P((D_n, D_{n+1}) = (d_n, d_{n+1})) = \frac{1}{100}.$$

The joint probability converges to $\frac{1}{100}$ very quickly as n increases. Intuitively, consider the 100 combinations of d_n and d_{n+1} for $n > 1$ as well as how quickly $\log_{10}(x)$ flattens. Of the 100 possible combinations, choose just the combinations such that $d_n = d_{n+1}$.

In other words, choose only matching pairs. Then

$$\lim_{n \rightarrow \infty} P(D_n = D_{n+1}) = \sum_{d=0}^9 \lim_{n \rightarrow \infty} P((D_n, D_{n+1}) = (d, d)) = \sum_{d=0}^9 \frac{1}{100} = \frac{1}{10}. \quad (4.4)$$

Thus, as n increases, the expected frequency of matched pairs of final digits in a Benford dataset approaches 10%.

[1,2]	[2,3]	[3,4]	[4,5]	[5,6]
0.1090508	0.1003304	0.1000035	0.1000000	0.1000000

Table 1: Probability of matched-pairs (i.e., last two digits are equal) in the $[n, (n+1)]$ digits. Digits [1, 2] cannot include 0.

As Table 1 illustrates, the aggregate probability of matched pairs, calculated via Equations (4.3) and (4.4), rapidly converges within the first few digits. Even starting at the second digit, the agreement is quite close. By the third digit the probability is off by only 0.00036%, and the probability differs by less than a factor of 10^{-7} after the fourth digit.

L2-BL 10 is based on this expected frequency of matched pairs, and specifically looks at the final two digits in each number for the sake of maximizing n . For L2-BL 10, this 10% frequency of observation of matched pair final digits acts as the null behavior and does not imply anything about the integrity of the data. Conversely, a statistically significant lack or over-abundance of matched-pairs in final digits could indicate that the data had been tampered.

4.2 Precinct-level data is well modeled the Discrete Weibull

[Kalktawi \(2017\)](#) conducted a study on the performance of the discrete Weibull with

under-dispersed and over-dispersed count data, as well as with count data with excessive zeros. That study found the discrete Weibull to be robust in all scenarios, and in simulations it modeled real and simulated data better than the Poisson distribution.

Figure 3 depicts the distributions of vote counts across Fulton County, Georgia; Genesee County, New York; and Walla Walla County, Washington from the 2016 U.S. Presidential Election (MIT Election Data and Science Lab, 2018). As can be seen, the data represent significantly skewed, heterogeneous vote count distributions within counties.¹ The robust performance of the discrete Weibull distribution under excessive zeros, under-dispersion, and over-dispersion in count data therefore makes it ideal for modeling precinct-level vote counts.

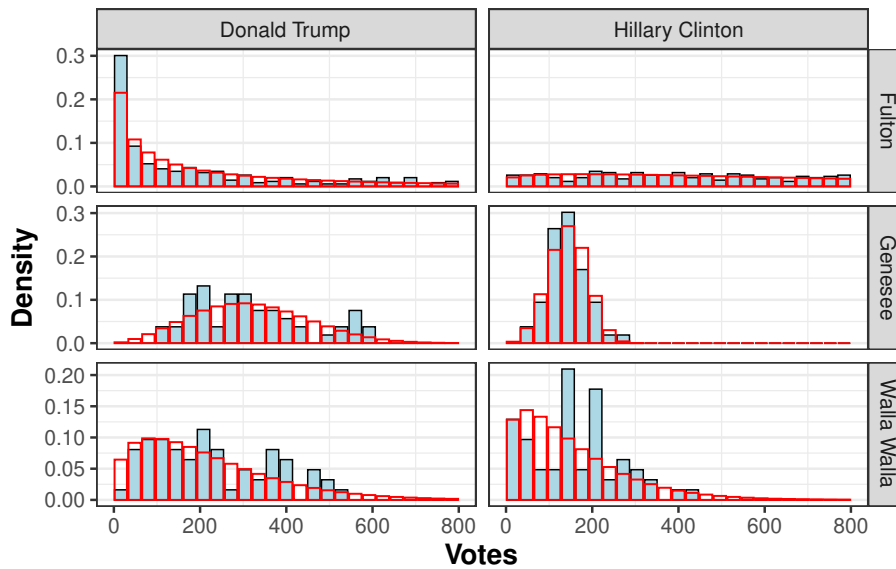


Figure 3: Distribution of Vote Counts in Genesee County, NY, Walla Walla County, WA, and Fulton County, GA in the 2016 U.S. Presidential Election. Estimated Weibull Distributions are Overlaid.

Table 2 presents $\hat{\mu}$, $\hat{\sigma}$, and d-KS test p -values for the counties displayed in Figure 3. Standard errors for the estimated parameters were calculated using the inverse of

¹A small number of precincts with over 800 votes were removed from the graph for visual clarity.

the Fisher information matrix. The low d-KS p-value associated with Walla Walla County for Clinton implies that the estimated Weibull distribution is poorly fit.

Trump						
	$\hat{\mu}_{i,j}$	$\mathbf{SE}_{\hat{\mu}}$	$\hat{\sigma}_{i,j}$	$\mathbf{SE}_{\hat{\sigma}}$	<i>p</i> -Value	N
Genesee County, NY	5.89	0.003	0.39	0.002	0.407	53
Walla Walla County, WA	5.47	0.009	0.73	0.006	0.803	62
Fulton County, GA	5.47	0.008	1.54	0.004	1	346
Clinton						
Genesee County, NY	5.08	0.002	0.28	0.001	0.89	53
Walla Walla County, WA	5.10	0.01	0.82	0.008	0.032	62
Fulton County, GA	6.74	0.002	0.873	0.037	0.79	346

Table 2: Weibull Parameters and d-KS Test Results for Selected Counties in the 2016 U.S. Presidential Election.

To demonstrate the practical ability of the discrete Weibull to model election data, we analyze all counties from the states represented in Figure 3. Additional analysis is available from the authors upon request. For each state and candidate, a discrete Weibull was modeled on the precinct vote counts of each county and d-KS tests were performed. These results are depicted in Figure 4.

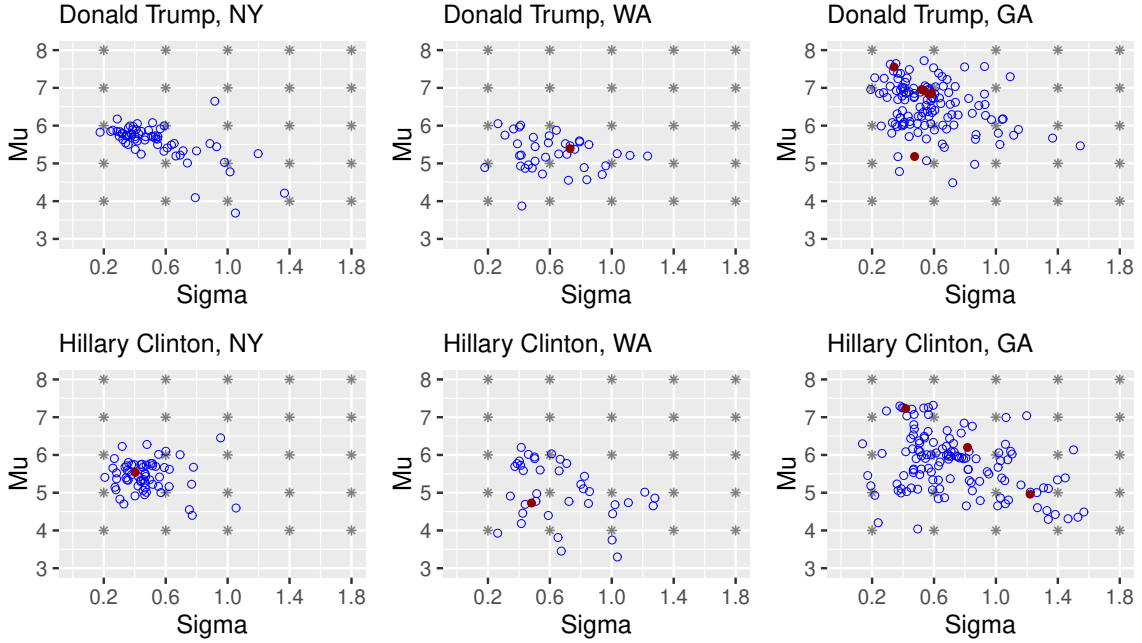


Figure 4: Results of d-KS Tests on Counties in Selected States in the 2016 U.S. Presidential Election. Cases where $p \leq 0.05$ Indicating Poorly Fit Estimated Distributions are Marked as Filled Circles.

Figure 4 maps the $\hat{\mu}$ and $\hat{\sigma}$ parameters of the estimated distributions of the counties on the Y and X axes respectively.² Un-filled points indicate counties with well fit distributions, and filled points indicate counties which had d-KS test p -values below 0.05 indicating poor fit. As Figure 4 illustrates, the richness of the Weibull distribution enables it to fit a wide array of vote count distributions. For a better understanding of the structural change of the discrete Weibull distribution over the parameter field, Figure 5 plots the discrete Weibull PMF as parameterized by the grid points marked with stars in Figure 4.

²Forsythe and Paulding Counties, GA for Donald Trump were removed for visual clarity. Forsythe County had $\hat{\mu} = 8.16$, $\hat{\sigma} = 0.83$, $p = 0.895$. Paulding County had $\hat{\mu} = 8.13$, $\hat{\sigma} = 0.3$, $p = 0.15$.

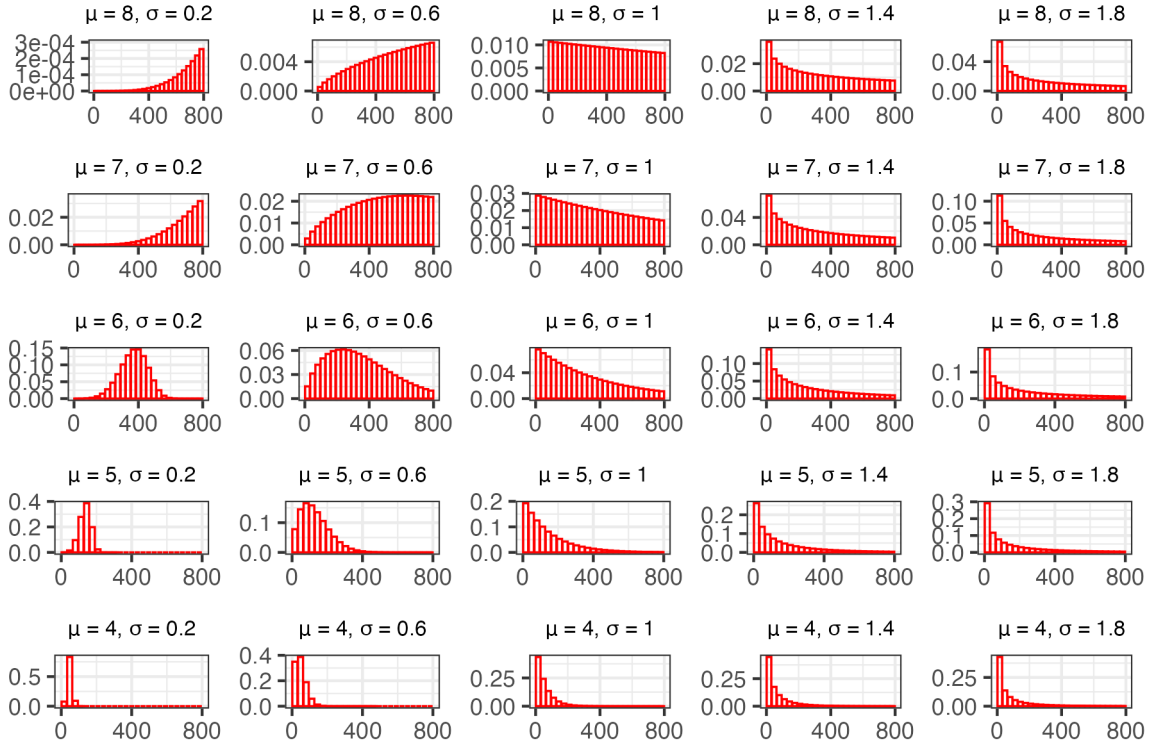


Figure 5: Discrete Weibull Probability Density Functions for a Variety of Parameterizations.

4.3 The Discrete Weibull Tends to Conform to L2-BL 10

Having established the discrete Weibull's effectiveness in modeling election data, we next examine its ability to reproduce Benford-consistent patterns by testing its conformity to L2-BL 10 across a grid of parameter values ($1 \leq \mu \leq 10$, $0.1 \leq \sigma \leq 2$). To assess this conformity, we utilize a chi-squared test with the null behavior being conformity. Accounting for the variability in precinct size, we conducted this demonstration using four realistic sample sizes. For each parameterization at each sample size, the chi-squared test was conducted as 100 Monte Carlo simulations. Figure 6 presents the results of those simulations and displays that L2-BL 10 holds across a wide range of discrete Weibull parameterizations and sample sizes.

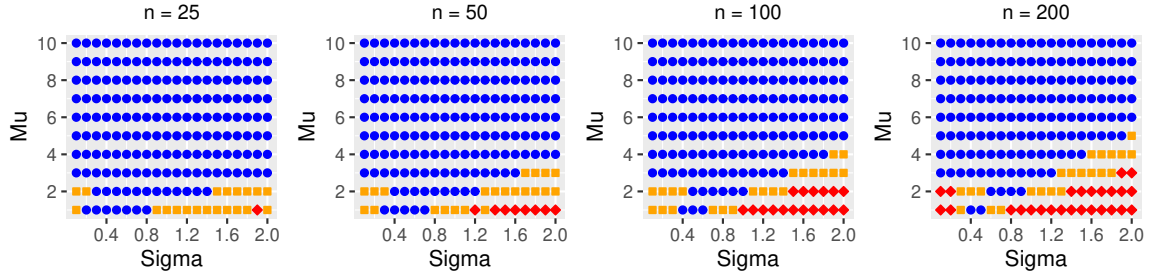


Figure 6: Results of L2-BL 10 Chi-Squared Test on Various Discrete Weibull Parameterizations. Cases where $p \leq 0.05$, Indicating Non-Adherence, are Marked as Diamonds. Cases where $0.05 < p \leq 0.1$ are Marked as Squares.

It should be noted, however, that adherence of the discrete Weibull to L2-BL 10 seems to degrade as the number of precincts increases. In the following section, we demonstrate L2-BL 10 analysis on nine states from the 2016 and 2020 U.S. Presidential Elections. Figure 7, containing by-county precinct count distributions across all states in each of those elections, shows that the degeneration of L2-BL 10 adherence with respect to precinct count is not a major concern. Furthermore, the locations of the points in Figure 4, if generalized, seem to indicate that a majority of Weibull parameterizations generated from fitting on real data fall within the L2-BL 10 adherent regions of Figure 6.

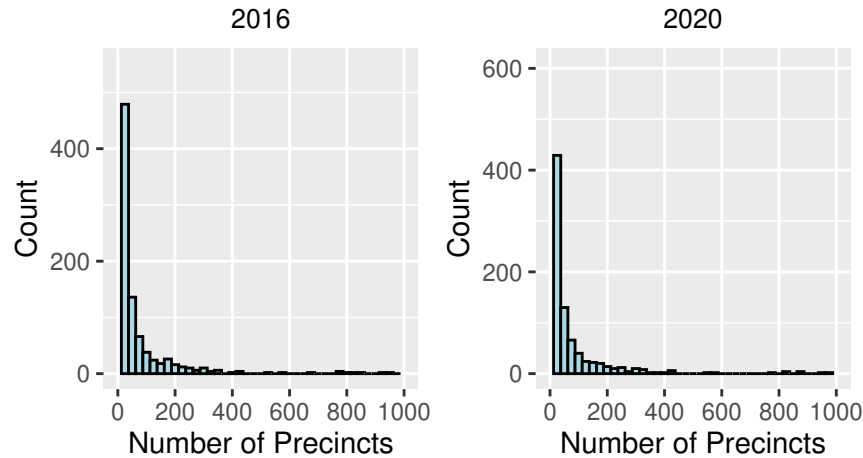


Figure 7: Distribution of County Precinct Counts Across Nine States from the 2016 and 2020 U.S. Presidential Elections.

5 Empirical Application to the 2016 and 2020 U.S. Presidential Elections

The effectiveness of modeling precinct-level vote count data with the discrete Weibull as well as the discrete Weibull’s general conformity to L2-BL 10 show the theoretical and practical ability of our methodology. We now present an empirical application of L2-BL 10.

In this section, we take data from nine states in the 2016 and 2020 U.S. Presidential elections ([MIT Election Data and Science Lab, 2022](#)). So as to fully display our method, we chose a group of states that included swing states as well as traditionally red or blue states. To prevent failures of our optimizer and reduce invalid results, we removed any counties with fewer than five precincts. In total, this accounts for 88 counties in 2016 and 118 counties in 2020. Additionally, because some states reported absentee votes aggregated to the county level instead of absentee vote counts for each

precinct, those states were filtered to only include in-person votes.³

To begin, we fit a discrete Weibull distribution onto each county and assessed the associated goodness of fit using one-sample bootstrap d-KS tests with 1000 bootstrap estimates. Fitting was done using the `optim` function from `stats` (R Core Team, 2024) for optimizing the negative sum of the log of the likelihood function, `ddweibull` from `dWeibullAlt` (Eigen, 2026), with respect to μ and σ . Initial values for μ and σ were set to 5 and 0.75, and lower bounds were set to -300 and 10^{-10} , respectively. A tiny constant was added to the likelihood function inside the logarithm so as to prevent errors caused by extremely small, positive probabilities being rounded to zero. d-KS test statistics were calculated using `KSgeneral` (Dimitrova et al., 2020), and the bootstrap procedure was conducted manually as described in Section 3. We then conducted chi-squared tests on the matched-pair frequencies in samples from the fitted distributions using 100 Monte Carlo simulations. Finally, we ran chi-squared tests on the observed data from every county. All tests used a significance level of $\alpha = 0.05$, and the chi-squared tests had their p -values adjusted via the Bonferroni correction for multiple comparisons. Tables 3 and 4 contain summary results from the study. *Well Fit* counties are those that did not have a statistically significant d-KS result. *Fully Flagged* counties are those with well fit estimated Weibulls which conformed with L2-BL 10, but their observed data did not. A list with parameters and test results for all fully-flagged counties is available in Appendix B.

³The states affected by this restriction were Florida, Pennsylvania, Tennessee, Nebraska, Missouri, and Maryland for 2016, and Florida, Pennsylvania, Tennessee, Nebraska, Missouri, and Washington in 2020.

State	Candidate	Total Counties	Well Fit	Fully Flagged
Florida	Clinton	67	66	1
	Trump		63	1
Georgia	Clinton	128	125	0
	Trump		122	1
Maryland	Clinton	24	23	1
	Trump		24	1
Missouri	Clinton	116	114	0
	Trump		112	0
Nebraska	Clinton	81	81	5
	Trump		81	8
New York	Clinton	62	61	3
	Trump		62	4
Pennsylvania	Clinton	67	67	0
	Trump		65	0
Tennessee	Clinton	94	92	1
	Trump		91	1
Washington	Clinton	39	38	3
	Trump		38	3
Total		1356	1325	33

Table 3: Results of Last Two Digit Base 10 Benford's Analysis on Select States in the 2016 U.S. Presidential Election.

State	Candidate	Total Counties	Well Fit	Fully Flagged
Florida	Biden	67	65	3
	Trump		64	2
Georgia	Biden	124	116	3
	Trump		116	0
Maryland	Biden	24	22	1
	Trump		24	1
Missouri	Biden	113	113	0
	Trump		112	0
Nebraska	Biden	74	74	2
	Trump		74	1
New York	Biden	62	62	0
	Trump		62	2
Pennsylvania	Biden	67	65	0
	Trump		66	0
Tennessee	Biden	94	89	1
	Trump		90	0
Washington	Biden	38	37	1
	Trump		38	0
Total		1326	1289	17

Table 4: Results of Last Two Digit Base 10 Benford’s Analysis on Select States in the 2020 U.S. Presidential Election.

As Tables 3 and 4 shows, of the nine states examined, seven states in 2016 and seven states in 2020 contained fully flagged counties. In total, 33 counties in 2016 and 17 counties in 2020 were fully flagged by this methodology and thus may warrant further investigation.

In practice, L2-BL 10 is most likely to be used on a single county. In that case, analysis would likely be stopped if the county was initially found to be conforming or if the distribution was poorly fit. For this study, we conducted all three steps on every county so as to observe the behavior of the test generally. Tables 5 and 6 provides

cross tabulations across all of the states and both candidates.

Weibull Fit	Fitted L2-BL 10	Observed L2-BL 10		
		Conforming	Non-Conforming	Total
Well Fit	Conforming	1291	33	1324
	Non-Conforming	0	0	0
	Total	1291	33	1324
Poorly Fit	Conforming	32	0	32
	Non-Conforming	0	0	0
	Total	32	0	32
Total	Conforming	1323	33	1356
	Non-Conforming	0	0	0
	Total	1323	33	1356

Table 5: Cross-Tabulations of L2-BL 10 Results in Nine States from the 2016 U.S. Presidential Election

Weibull Fit	Fitted L2-BL 10	Observed L2-BL 10		
		Conforming	Non-Conforming	Total
Well Fit	Conforming	1273	17	1290
	Non-Conforming	0	2	2
	Total	1273	19	1292
Poorly Fit	Conforming	34	0	34
	Non-Conforming	0	0	0
	Total	34	0	34
Total	Conforming	1307	17	1324
	Non-Conforming	0	2	2
	Total	1307	19	1326

Table 6: Cross-Tabulations of L2-BL 10 Results in Nine States from the 2020 U.S. Presidential Election

6 Conclusions and Future Research

This study presents a novel adaptation of Benford’s Law as a digit-based tool for election forensics. Although first- and second-digit base-10 tests are widely used, these methods are known to perform poorly when applied to clustered data, a common feature of precinct-level election returns (Anderson et al., 2022). Some researchers have attempted to address this limitation through base transformations that artificially expand the range of values. By contrast, the L2-BL 10 approach avoids this issue entirely by focusing on the distribution of final digit pairs, eliminating the need for data to span multiple orders of magnitude.

By analyzing the distributional properties of precinct-level vote counts through a Benford-based framework and modeling them with the discrete Weibull distribution, we develop a statistically grounded method for identifying irregular patterns in precinct level data. Applying L2-BL 10 to county-level data from nine states in the 2016 and 2020 U.S. presidential elections, the procedure flagged 50 counties whose digit patterns deviated from expected Benford behavior. Such deviations are consistent with potential irregularities but do not, by themselves, establish mechanism, intent, or evidence of malfeasance. Accordingly, L2-BL 10 is best interpreted as a diagnostic indicator to be used in conjunction with other forensic tools, including mixture modeling, Bayesian anomaly detection, and multimodal vote distribution analysis (Lenk and DeSarbo, 2000; Anderson et al., 2022; Klimek et al., 2012).

A fundamental feature of L2-BL 10 is that it preserves the accessibility that has long made Benford-based methods appealing. Whereas traditional first-digit analyses often require careful interpretation, the near-uniform distribution of matched final digits under L2-BL 10 is both intuitive and statistically transparent. This clarity en-

hances the method’s usefulness not only for researchers and election officials, but also for journalists, watchdog organizations, and other members of the public interested in examining electoral data using readily available information.

L2-BL 10 adds an innovative, novel, and interpretable tool to the continually growing toolbox of methods used in the analysis of election integrity. Future work can assess its performance across a broader range of settings, including earlier U.S. presidential elections, state and local contests, and international cases such as the 2004 Ukrainian presidential election (Myagkov et al., 2009; Mebane Jr, 2008, 2019). Future work can also study the effect on L2-BL 10 of disaggregation versus combination of in-person and absentee votes, election-day and early votes, or other combinations of voting modes where anomalies may appear more frequently through one mode than the other. In Section 5, we had to include only in-person votes for certain states as a result of how the data were reported. It is possible that important signals were removed, signals irrelevant to in-person votes were removed, or signals unique to in-person votes were revealed. A framework for parallel or joint testing could be developed. The framework may also extend to related questions of political data integrity, such as the analysis of campaign finance records, where deviations from expected digit patterns could signal irregular reporting.

The applications of the technique presented in this study can extend beyond simply electoral contexts. For example, in scientific research, the approach may aid in detecting irregularities in datasets whose values lie within relatively narrow ranges, where traditional Benford analyses are less effective. In financial auditing, digit-level diagnostics could help identify fabricated or inflated values that escape detection under first-digit tests. Similar logic may apply in sports analytics—for example,

in the examination of statistics such as earned run averages or batting averages in baseball—where unexpected digit patterns could prompt closer scrutiny of reported performance data.

In sum, L2-BL 10 represents a practical extension of a well-known statistical principle. By retaining the interpretability of Benford-based methods while addressing key structural limitations through distributional modeling, it offers a useful addition to the set of tools available for evaluating both electoral and non-electoral data.

Declaration of conflicting interests

The authors declared no potential conflicts of interest with respect to the research, authorship and/or publication of this article.

References

- Anderson, K. M., Dayaratna, K., Gonshorowski, D., and Miller, S. J. (2022). A new benford test for clustered data with applications to american elections. *Stats*, **5**(3), 841–855. doi:[10.3390/stats5030049](https://doi.org/10.3390/stats5030049).
- Arshadi, L. and Jahangir, A. H. (2014). Benford's law behavior of internet traffic. *Journal of Network and Computer Applications*, **40**, 194–205. doi:[10.1016/j.jnca.2013.09.007](https://doi.org/10.1016/j.jnca.2013.09.007).
- Beber, B. and Scacco, A. (2012). What the numbers say: A digit-based test for election fraud. *Political Analysis*, **20**(2), 211–234. doi:[10.1093/pan/mps003](https://doi.org/10.1093/pan/mps003).
- Benford, F. (1938). The law of anomalous numbers. *Proceedings of the Ameri-*

can philosophical society, pages 551–572. URL <http://www.jstor.org/stable/984802>.

Berger, A. and Hill, T. P. (2015). *A Short Introduction to the Mathematical Theory of Benford's Law*, chapter 2, pages 23–67. Princeton University Press. doi:10.2307/j.ctt1dr358t.7.

Castaneda, G. (2010). La ley de benford y su aplicabilidad en el análisis forense de resultados electorales. *Política y Gobierno*, **18**, 297–329. URL <http://www.politicaygobierno.cide.edu/index.php/pyg/article/view/158>.

City of Forest Acres (2021). 2021 general election. URL <https://www.forestacres.net/news/2021-general-election-city-council-updated-official-results>.

Collection, Y. P. (1840). *The Politician's Register*. G.H. Hickman. URL <https://www.loc.gov/resource/gdcmassbookdig.politiciansregis00yapa/?sp=16&st=image&r=-1.399,0.054,3.798,1.577,0>.

Conover, W. J. (1972). A kolmogorov goodness-of-fit test for discontinuous distributions. *Journal of the American Statistical Association*, **67**(339), 591–596. ISSN 01621459. doi:10.2307/2284444.

Deckert, J., Myagkov, M., and Ordeshook, P. C. (2011). Benford's law and the detection of election fraud. *Political Analysis*, **19**(3), 245–268. doi:10.1093/pan/mpr014.

Dickenson, J. R. (1984). Republican declared winner of house race in indiana. URL <https://www.washingtonpost.com/archive/politics/1984/12/15/republican-declared-winner-of-house-race-in-indiana/91c3fd5f-3e4e-4475-b037-a336ef77482b>.

- Dimitrova, D. S., Kaishev, V. K., and Tan, S. (2020). Computing the Kolmogorov-Smirnov distribution when the underlying CDF is purely discrete, mixed, or continuous. *Journal of Statistical Software*, **95**(10), 1–42. doi:[10.18637/jss.v095.i10](https://doi.org/10.18637/jss.v095.i10).
- Eigen, P. (2026). *dWeibullAlt: Provides Stats Package Like Support for Alternative Discrete Weibull Parameterizations*. URL <https://github.com/Philiprex/dWeibullAlt>. R package version 0.0.0.9000, commit 5ae58d3dda2c8c1b36b63f22d7522ab04612c2cb.
- Englehardt, J. D. and Li, R. (2011). The discrete weibull distribution: an alternative for correlated counts with confirmation for microbial counts in water. *Risk Analysis: An International Journal*, **31**(3), 370–381. doi:[10.1111/j.1539-6924.2010.01520.x](https://doi.org/10.1111/j.1539-6924.2010.01520.x).
- Fiar, J. L., Goldaman, T., and Perez-Mercader, J. (2012). Genome sizes and the benford distribution. *PLoS ONE*, **7**(5). doi:[10.1371/journal.pone.0036624](https://doi.org/10.1371/journal.pone.0036624).
- Geyer, A. and Martí, J. (2012). Applying benford’s law to volcanology. *Geology*, **40**(4), 327–330. doi:[10.1130/G32787.1](https://doi.org/10.1130/G32787.1).
- Gleser, L. J. (1985). Exact power of goodness-of-fit tests of kolmogorov type for discontinuous distributions. *Journal of the American Statistical Association*, **80**(392), 954–958. ISSN 01621459. doi:[10.2307/2288560](https://doi.org/10.2307/2288560).
- Grammatikos, T. and Papanikolaou, N. I. (2021). Applying benford’s law to detect accounting data manipulation in the banking industry. *Journal of Financial Services Research*, **59**(1), 115–142. doi:[10.1007/s10693-020-00334-9](https://doi.org/10.1007/s10693-020-00334-9).
- Henze, N. (1996). Empirical-distribution-function goodness-of-fit tests for discrete models. *Canadian Journal of Statistics*, **24**(1), 81–93. doi:[10.2307/3315691](https://doi.org/10.2307/3315691).

Jiménez, R. and Hidalgo, M. (2014). Forensic analysis of venezuelan elections during the Chávez presidency. *PloS one*, **9**(6), e100884. doi:[10.1371/journal.pone.0100884](https://doi.org/10.1371/journal.pone.0100884).

Jolion, J.-M. (2001). Images and benford's law. *Journal of Mathematical Imaging and Vision*, **14**(1), 73–81. doi:[10.1023/A:1008363415314](https://doi.org/10.1023/A:1008363415314).

Kalktawi, H. S. (2017). *Discrete Weibull Regression Model for Count Data*. PhD thesis, Brunel University of London. URL <http://bura.brunel.ac.uk/handle/2438/14476>.

Klimek, P., Yegorov, Y., and Thurner, S. (2012). Statistical detection of systematic election irregularities. *Proceedings of the National Academy of Sciences*, **109**(41), 16469–16473. doi:[10.1073/pnas.1210722109](https://doi.org/10.1073/pnas.1210722109).

Lakshmanan, K. (2024). The 2018 russian presidential election. doi:[10.2139/ssrn.4957116](https://doi.org/10.2139/ssrn.4957116).

Lenk, P. J. and DeSarbo, W. S. (2000). Bayesian inference for finite mixtures of generalized linear models with random effects. *Psychometrika*, **65**(1), 93–119. doi:[10.1007/BF02294188](https://doi.org/10.1007/BF02294188).

Mebane Jr, W. R. (2006). Election forensics: Vote counts and benford's law. In *Summer Meeting of the Political Methodology Society, UC-Davis, July*, volume 17. URL <https://websites.umich.edu/~wmebane/pm06.pdf>.

Mebane Jr, W. R. (2008). Election forensics: Outlier and digit tests in america and russia. In *American Electoral Process conference, Center for the Study of Democratic Politics, Princeton University*. URL <https://websites.umich.edu/~wmebane/aep2008.pdf>.

- Mebane Jr, W. R. (2010). Fraud in the 2009 presidential election in iran? *Chance*, **23**(1), 6–15. doi:[10.1007/s00144-010-0003-4](https://doi.org/10.1007/s00144-010-0003-4).
- Mebane Jr, W. R. (2011). Comment on 'benford's law and the detection of election fraud'. *Political Analysis*, **19**(3), 269–272. doi:[10.1093/pan/mpr024](https://doi.org/10.1093/pan/mpr024).
- Mebane Jr, W. R. (2012). Second-digit tests for voters' election strategies and election fraud. In *Annual Meeting of the Midwest Political Science Association, Chicago*. Citeseer. URL <https://websites.umich.edu/~wmebane/mw12.pdf>.
- Mebane Jr, W. R. (2019). Evidence against fraudulent votes being decisive in the bolivia 2019 election. URL <https://websites.umich.edu/~wmebane/Bolivia2019.pdf>.
- Mebane Jr., W. R. (2023). Lost votes and posterior multimodality in the eforensics model. In *Annual Meeting of the Society for Political Methodology, Stanford University*. URL <https://websites.umich.edu/~wmebane/pm23.pdf>.
- Mikoss, I. (2004). Evidencia de manipulación artificial de los resultados al aplicar la ley de benford al referedum venezolano de agosto de 2004. Technical report, Universidad Simón Bolívar, Valle de Sartenejas, Departamento de Física. URL https://urru.org/papers/200408_en_adelante_Fraude.htm. PDF archived on URRU.org, curated by Iruña Urruticoechea.
- Miller, S. J. (2015). *A Quick Introduction to Benford's Law*, chapter 1, pages 3–22. Princeton University Press. doi:[10.2307/j.ctt1dr358t.6](https://doi.org/10.2307/j.ctt1dr358t.6).
- MIT Election Data and Science Lab (2018). U.s. president precinct-level returns 2016. URL <https://doi.org/10.7910/DVN/LYWX3D>.

MIT Election Data and Science Lab (2022). U.s. president precinct-level returns 2020.

URL <https://doi.org/10.7910/DVN/JXPRES>.

Myagkov, M., Ordeshook, P. C., and Shakin, D. (2009). *Ukraine 2004*, page 138–182.

Cambridge University Press. doi:[10.1017/CBO9780511626807](https://doi.org/10.1017/CBO9780511626807).

Nakagawa, T. and Osaki, S. (1975). The discrete weibull distribution. *IEEE trans-*

actions on reliability, **24**(5), 300–301. doi:[10.1109/TR.1975.5214915](https://doi.org/10.1109/TR.1975.5214915).

Newcomb, S. (1881). Note on the frequency of use of the different digits in natural

numbers. *American Journal of mathematics*, **4**(1), 39–40. doi:[10.2307/2369148](https://doi.org/10.2307/2369148).

Niederhausen, H. (1981). Sheffer polynomials for computing exact kolmogorov-

smirnov and renyi type distributions. *The Annals of Statistics*, **9**.

doi:[10.1214/aos/1176345574](https://doi.org/10.1214/aos/1176345574).

Nigrini, M. J. and Miller, S. J. (2007). Benford’s law applied to hydrology

data—results and relevance to other geophysical data. *Mathematical Geology*, **39**

(5), 469–490.

Patriarca, R., Hu, T., Costantino, F., Di Gravio, G., and Tronci, M. (2019). A

system-approach for recoverable spare parts management using the discrete weibull

distribution. *Sustainability*, **11**(19), 5180. doi:[10.3390/su11195180](https://doi.org/10.3390/su11195180).

Peluso, A., Vinciotti, V., and Yu, K. (2019). Discrete weibull generalized additive

model: An application to count fertility data. *Journal of the Royal Statistical Soci-*

ety: Series C (Applied Statistics), **68**(3), 565–583. doi:[10.48550/arXiv.1801.07905](https://doi.org/10.48550/arXiv.1801.07905).

Pericchi, L. R. and Torres, D. (2004). La ley de newcomb-benford y sus apli-

caciones al referendum revocatorio en venezuela. Reporte técnico no-definitivo,

- 2a versión, Universidad de Puerto Rico and Universidad Simón Bolívar. URL https://urru.org/papers/200408_en_adelante_Fraude.htm. PDF archived on URRU.org, curated by Iruña Urruticoechea.
- R Core Team (2024). *R: A Language and Environment for Statistical Computing*. R Foundation for Statistical Computing, Vienna, Austria. URL <https://www.R-project.org/>.
- Stute, W., Manteiga, W. G., and Quindimil, M. P. (1993). Bootstrap based goodness-of-fit-tests. *Metrika*, **40**, 243–256. doi:[10.1007/BF02613687](https://doi.org/10.1007/BF02613687).
- Villas-Boas, S. B., Fu, Q., and Judge, G. (2017). Benford’s law and the fsd distribution of economic behavioral micro data. *Physica A: Statistical Mechanics and Its Applications*, **486**, 711–719. doi:[10.1016/j.physa.2017.05.093](https://doi.org/10.1016/j.physa.2017.05.093).
- Zhang, M., Alvarez, R. M., and Levin, I. (2019). Election forensics: Using machine learning and synthetic data for possible election anomaly detection. *PloS one*, **14** (10), e0223950. doi:[10.1371/journal.pone.0223950](https://doi.org/10.1371/journal.pone.0223950).

A Proof of L2-BL 10

Theorem 1. Equation (2.3) from [Berger and Hill \(2015\)](#) describes Benford's Law as the joint probability

$$\begin{aligned} P((D_1, D_2, \dots, D_m) = (d_1, d_2, \dots, d_m)) \\ = \log_{10} \left(1 + \left(\sum_{j=1}^m 10^{m-j} d_j \right)^{-1} \right) \end{aligned}$$

for all positive integers m where D_i is the value of the i_{th} digit of the significand and $D_1 \geq 1$. Then

$$\lim_{n \rightarrow \infty} P((D_n, D_{n+1}) = (d_n, d_{n+1})) = \frac{1}{100}.$$

Proof. Given

$$\begin{aligned} P((D_1, D_2, \dots, D_m) = (d_1, d_2, \dots, d_m)) \\ = \log_{10} \left(1 + \left(\sum_{j=1}^m 10^{m-j} d_j \right)^{-1} \right), \end{aligned}$$

we can find the probability of just the n_{th} digit by first isolating d_n as such

$$\begin{aligned} P((D_1, D_2, \dots, D_n) = (d_1, d_2, \dots, d_n)) \\ = \log_{10} \left(1 + \left(\sum_{j=1}^n 10^{n-j} d_j \right)^{-1} \right) \\ = \log_{10} \left(1 + \left(\sum_{j=1}^{n-1} (10^{n-1-j} d_j) + d_n \right)^{-1} \right) \\ = \log_{10} \left(1 + \left(10 \sum_{j=1}^{n-1} (10^{n-2-j} d_j) + d_n \right)^{-1} \right) \\ = \log_{10} \left(1 + \left(10k + d_n \right)^{-1} \right), \end{aligned}$$

and then summing the log over all possible values of k . Factoring 10 out of the sum makes iterating over the bounds of k easier. Now, k can be any $n - 1$ digit number with $D_1 \geq 1$, making $10k + d_n$ an n digit number with $D_1 \geq 1$ and $D_n = d_n$. So the bounds of k are $[10^{n-2}, 10^{n-1} - 1] \subset \mathbb{N}$, and

$$P(D_n = d_n) = \sum_{k=10^{n-2}}^{10^{n-1}-1} \log_{10} \left(1 + \frac{1}{10k + d_n} \right).$$

We can find, through the same process, the joint probability of D_n and D_{n+1} :

$$\begin{aligned} P((D_1, D_2, \dots, D_n, D_{n+1}) = (d_1, d_2, \dots, d_n, d_{n+1})) \\ &= \log_{10} \left(1 + \left(\sum_{j=0}^{n+1} 10^{n+1-j} d_j \right)^{-1} \right) \\ &= \log_{10} \left(1 + \left(100k + 10d_n + d_{n+1} \right)^{-1} \right). \end{aligned}$$

Again, factoring out 100 allows k to be an $n - 1$ digit number with $D_1 \geq 1$ so that $100k + 10d_n + d_{n+1}$ is an $n + 1$ digit number with $D_1 \geq 1$, $D_n = d_n$, and $D_{n+1} = d_{n+1}$. So,

$$P((D_n, D_{n+1}) = (d_n, d_{n+1})) = \sum_{k=10^{n-2}}^{10^{n-1}-1} \log_{10} \left(1 + \frac{1}{100k + 10d_n + d_{n+1}} \right).$$

We use the Taylor expansion $\log(1 + x) = x - x^2/2 + x^3/3 + \dots$ to approximate $\log(1 + x) = x + O(x^2)$ where $x = \frac{1}{100k + 10d_n + d_{n+1}}$. Here $O(x^2)$ is big-Oh notation and represents an error of at most Cx^2 for some positive constant C and large x . Our

error is on the order of $\frac{1}{10^n}$, and so gets extremely small as n increases.

$$\begin{aligned} P((D_n, D_{n+1}) = (d_n, d_{n+1})) &= \frac{1}{\log(10)} \sum_{k=10^{n-2}}^{10^{n-1}-1} \log \left(1 + \frac{1}{100k + 10d_n + d_{n+1}} \right) \\ &\approx \frac{1}{\log(10)} \sum_{k=10^{n-2}}^{10^{n-1}-1} \frac{1}{100k + 10d_n + d_{n+1}}. \end{aligned}$$

We also approximate the sums as integrals, again introducing a small error.⁴ Naturally, this error also decreases rapidly with n .

$$\begin{aligned} P((D_n, D_{n+1}) = (d_n, d_{n+1})) &\approx \frac{1}{\log(10)} \sum_{k=10^{n-2}}^{10^{n-1}-1} \frac{1}{100k + 10d_n + d_{n+1}} \\ &\approx \frac{1}{\log(10)} \int_{k=10^{n-2}}^{10^{n-1}-1} \frac{1}{100k + 10d_n + d_{n+1}} dk \\ &\approx \frac{1}{100 \log(10)} \left[\log \left(100(10^{n-1} - 1) + 10d_n + d_{n+1} \right) - \right. \\ &\quad \left. \log \left(100(10^{n-2}) + d_n + d_{n+1} \right) \right] \\ &\approx \frac{1}{100 \log(10)} \left[\log \left(10^{n+1} - 100 + 10d_n + d_{n+1} \right) - \right. \\ &\quad \left. \log \left(10^n + 10d_n + d_{n+1} \right) \right] \\ &\approx \frac{1}{100 \log(10)} \log \left(\frac{10^{n+1} - 100 + 10d_n + d_{n+1}}{10^n + 10d_n + d_{n+1}} \right). \end{aligned}$$

⁴The error is on the order of the size of the largest or smallest term when we have a sum that is monotonic, as we do here; thus our error is on the order of $\frac{1}{10^{n-2}}$.

At this point we can evaluate the limit.

$$\begin{aligned}
\lim_{n \rightarrow \infty} P((D_n, D_{n+1}) = (d_n, d_{n+1})) &\approx \lim_{n \rightarrow \infty} \left[\frac{1}{100 \log(10)} \log \left(\frac{10^{n+1} - 100 + 10d_n + d_{n+1}}{10^n + 10d_n + d_{n+1}} \right) \right] \\
&\approx \frac{1}{100 \log(10)} \log \left(\lim_{n \rightarrow \infty} \frac{10^{n+1} - 100 + 10d_n + d_{n+1}}{10^n + 10d_n + d_{n+1}} \right) \\
&\approx \frac{1}{100 \log(10)} \log \left(\lim_{n \rightarrow \infty} \frac{10^{n+1}}{10^n} \right) \\
&\approx \frac{1}{100 \log(10)} \log(10) \\
&\approx \frac{1}{100}.
\end{aligned}$$

□

B Empirical Study Results

State	Candidate	County	N	Obs χ^2 adj. p	$\hat{\mu}$	SE_{μ}	$\hat{\sigma}$	SE_{σ}	d-KS p	Fit χ^2 adj. p	
FL	Clinton	Brevard	170	0.0009	6.4385	0.0115	1.3498	0.0088	1	31.5421	
	Trump	Miami-Dade	858	0.0001	5.8696	0.002	1.2589	0.0014	1	32.4492	
GA	Trump	Madison	12	0.0327	6.7165	0.0328	0.5954	0.0193	0.396	64.6864	
MD	Clinton	Prince George's	302	0	6.2813	0.0048	1.1682	0.0041	1	11.5968	
	Trump	Prince George's	302	0	4.0412	0.0066	1.3457	0.0044	0.999	5.5974	
NE	Clinton	Boyd	5	0	2.7564	1.1367	2.1894	1.2735	0.982	23.7465	
		Cheyenne	11	0.0001	3.6766	0.1411	1.1948	0.1204	0.837	45.0936	
		Colfax	9	0.0464	3.1351	1.4522	3.2551	1.6154	0.98	13.7156	
		Morrill	11	0.0001	2.8316	0.2638	1.6019	0.2327	0.835	31.4198	
		Webster	7	0.0026	3.3254	0.4214	1.6258	0.4228	0.967	35.2514	
		Trump	Boone	13	0.0011	4.557	0.4816	2.3617	0.5071	0.998	25.2628
			Colfax	9	0.0004	3.8981	2.0905	3.9096	2.3912	1	16.2792
			Dodge	37	0.0051	5.4358	0.0298	1.0275	0.0285	1	40.5114
			Kimball	7	0.0026	4.6282	0.7045	2.11	0.747	0.987	30.2982
			Polk	8	0.0132	5.2362	0.2112	1.2593	0.1952	0.988	37.5671
			Sherman	8	0.0001	4.7637	0.4049	1.7289	0.4455	0.999	38.8383
			Thayer	9	0.0464	5.1697	0.2189	1.3612	0.2078	0.993	41.0125
			Wayne	13	0.0011	5.0025	0.2188	1.6276	0.2402	1	35.1003
	NY	Clinton	Nassau	1202	0	5.6743	0.0005	0.7794	0.0004	1	31.7521
			New York	1168	0.0006	6.2772	0.0002	0.4789	0.0002	1	28.695
		Queens	1255	0.0125	6.0973	0.0003	0.6007	0.0002	1	29.6287	
		Trump	Bronx	937	0.0116	3.685	0.0013	1.0504	0.0006	1	24.3341
			Jefferson	69	0.0162	5.8735	0.0038	0.4888	0.0023	0.678	32.2756
			Nassau	1202	0	5.5239	0.0007	0.8858	0.0005	1	35.6678
		Queens	1255	0	4.7773	0.0009	1.0155	0.0006	1	30.2559	
TN	Clinton	Dyer	17	0.0478	5.142	0.0537	0.9151	0.0327	0.721	43.3373	
	Trump	Macon	11	0.0083	6.3814	0.0435	0.6861	0.0444	1	50.7215	
WA	Clinton	Benton	244	0	4.6811	0.0046	1.0211	0.0038	1	19.3788	
		Kitsap	210	0.0218	5.7738	0.0025	0.7088	0.0018	1	20.8629	
		Mason	39	0.0441	5.8382	0.0045	0.403	0.0029	0.724	20.6742	
WA	Trump	Benton	244	0.0002	5.2578	0.0047	1.0346	0.0039	1	18.0017	
		Franklin	104	0.0003	4.8887	0.0071	0.8215	0.0044	0.638	20.9426	
		Wahkiakum	11	0.0035	4.9309	0.0172	0.4106	0.0085	0.983	19.6258	

Table 7: Details of Counties Fully Flagged by L2-BL 10 from Nine States in the 2016 U.S. Presidential Election.

State	Candidate	County	N	Obs χ^2 adj. p	$\hat{\mu}$	SE_{μ}	$\hat{\sigma}$	SE_{σ}	d-KS p	Fit χ^2 adj. p
FL	Biden	Brevard	171	0.0265	6.6555	0.011	1.3229	0.0082	1	30.2564
		Miami-Dade	866	0	6.5407	0.0015	1.0989	0.0011	1	35.5731
		Palm Beach	872	0	6.0005	0.0031	1.5925	0.0026	1	17.2405
	Trump	Miami-Dade	866	0.0005	6.3372	0.0019	1.2411	0.0014	1	34.6133
		Palm Beach	872	0	5.7441	0.003	1.5501	0.0023	1	19.8515
GA	Biden	Elbert	11	0.011	5.561	0.1064	1.0155	0.046	0.758	66.9579
		Habersham	7	0.004	6.338	0.0738	0.6796	0.0408	0.159	52.8547
		Peach	7	0.004	6.8507	0.0506	0.5698	0.0351	0.852	55.1223
MD	Biden	Prince George's	303	0	7.0549	0.0057	1.2759	0.0048	1	11.6387
	Trump	Prince George's	303	0.0001	4.7163	0.0056	1.2481	0.004	1	11.8354
NE	Biden	Gosper	5	0.0144	3.5935	0.4616	1.4458	0.3747	0.156	27.0177
		Harlan	9	0	3.5334	0.0471	0.6341	0.0398	0.886	46.3534
		Trump	Howard	9	0.0423	5.7337	0.1199	1.0123	0.0991	0.978
NY	Trump	Greene	52	0.0193	5.7383	0.0036	0.4098	0.0021	0.761	29.4018
		Queens	1393	0.0001	5.0805	0.0006	0.8501	0.0003	1	29.8169
TN	Biden	Hamilton	135	0.0008	6.2778	0.0105	1.1432	0.0074	1	44.281
WA	Biden	Benton	245	0.0001	5.0431	0.0051	1.0775	0.0041	1	18.6453

Table 8: Details of Counties Fully Flagged by L2-BL 10 from Nine States in the 2020 U.S. Presidential Election.